Supporting Information for

Air-stable chiral double-decker Dy(III) macrocycles with fluoride ion as the sole axial ligand

Xiaodong Liu,[a, b] Chen Zhao,[a, b] Jinjiang Wu,[a, b] Zhenhua Zhu[a, c] and Jinkui Tang*[a, b]

[a] State Key Laboratory of Rare Earth Resource Utilization, Changchun Institute of Applied Chemistry, Chinese Academy of Sciences, Changchun 130022. E-mail: tang@ciac.ac.cn;

[b] School of Applied Chemistry and Engineering, University of Science and Technology of China, Hefei 230026

[c] University of Chinese Academy of Sciences, Beijing 100049

Contents

1. Synthesis and Characterization

General Procedure

All manipulations described below were performed under aerobic conditions. The precursor complexes, **1-P** and **2-P**, were prepared in excellent yields according to a reported method.[1] Other reagents were purchased from commercial sources and used as received without further purification.

Measurements

Elemental analyses (C, H, N) were performed on a Perkin-Elmer 2400 analyzer. FT-IR spectra were recorded with a Nicolet 6700 Flex FTIR spectrometer equipped with a smart iTR attenuated total reflectance (ATR) sampling accessory in the range from 4000 to 530 cm^{-1}. Powder X-ray diffraction (PXRD) measurements were recorded on Bruker D8 advance X-Ray diffractometer using Cu-Kα radiation. The circular dichroism (CD) spectra data were collected on a Chirascan CD spectrometer (Applied Photophysics) at room temperature with scanning speed of 1 nm/s. Thermogravimetric analyses (TGA) were performed on a Netzsch STA449F3 TG-DSC instrument with a nitrogen atmosphere in the range of 30-800 ºC with a heating rate of 10 K min^{-1}. All magnetic susceptibility measurements were carried on a Quantum Design MPMS-XL7 magnetometer equipped with a 7 T magnet. Single Crystal X-Ray diffraction data were collected using a Bruker Apex III CCD diffractometer with graphite-monochromated Mo Kα radiation (α = 0.71073 Å) at 180 K. Direct-current (dc) magnetic susceptibility measurements were collected with an external dc magnetic field of 1000 Oe in the temperature range of 2-300 K. The experimental magnetic susceptibility data were corrected for the diamagnetism estimated from Pascal's tables and sample holder calibration.[2] Alternative-current (ac) magnetic susceptibility data were collected in a zero dc field with a 3.0 Oe ac oscillating field in the temperature range 2-30 K.

Synthesis

Synthesis Procedure for 1

The precursor **1-P** (324 mg, 0.4 mmol) and sodium tetraphenylboron (137 mg, 0.4 mmol) was added to a solution of NaF (101 mg, 2.4 mmol) in 40 mL DCM and 40 mL deionized water. The solution was then heated to reflux at 80°C for 20 minutes. After cooling to room temperature, the organic phase was separated and filtered. Yellow crystals of **1** suitable for single-crystal X-ray measurement were obtained by the slow diffusion of n-hexane into above organic phase at room temperature for two days, affording a reproducible yield (34 mg, 7 % based on Dy). Elemental analysis (%) calcd for $C_{134}H_{112}B_2Cl_4Dy_2F_4N_{12}$ (M_W = 2454.66): C, 65.56; H, 4.60; N, 6.85. Found: C, 65.80; H, 4.65; N, 6.88. FTIR ν / cm^{-1} (ART): 540 (s), 579 (s), 606 (s), 698 (s), 733 (m), 760 (m), 806 (m), 847 (m), 964 (m), 1009 (m), 1032 (m), 1072 (w), 1163 (m), 1265 (m), 1377 (m), 1454 (m), 1591 (m), 1651 (m), 3032 (m).

Synthetic Procedure for 2

The synthetic procedure of **2** is similar to that of **1**. Yield = 30 mg, (6% based on Dy). Elemental analysis (%) calcd for $C_{134}H_{114}B_2Cl_4Dy_2F_4N_{12}O_1$ (M_W = 2472.67): C, 65.08; H, 4.65; N, 6.80. Found: C, 64.95; H, 4.549; N, 6.83. FTIR ν/cm^{-1} (ART): 532 (s), 548 (s), 579 (s), 613 (m), 698 (s), 733 (m), 762 (m), 806 (m), 847 (m), 966 (m), 1009 (m), 1032 (m), 1066 (w), 1163 (m), 1269 (m), 1375 (m), 1454 (m), 1591 (m), 1653 (m), 3030 (m).

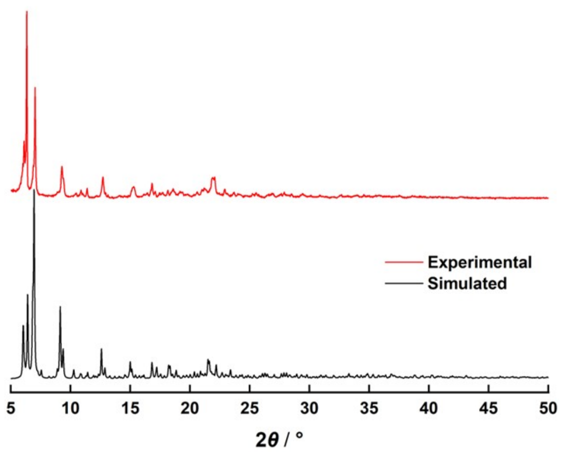

Fig. S1 PXRD data of **1**.

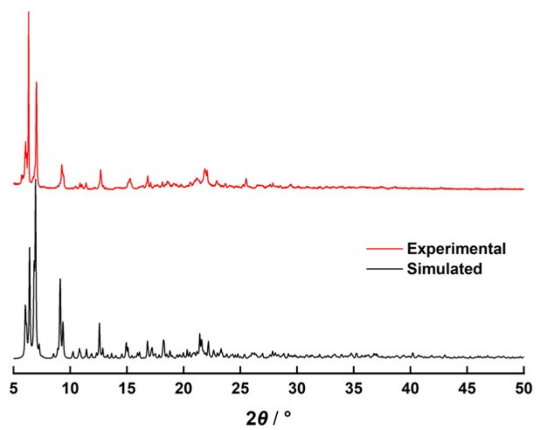

Fig. S2 PXRD data of **2**.

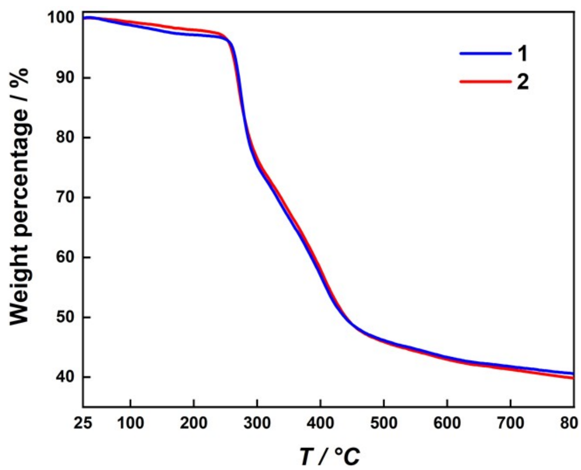

Fig. S3 Thermogravimetric analyses of **1 (**blue line) and **2** (red line).

2. Single-crystal X-ray Crystallography

The structures of **1** and **2** were solved in Olex2 with SHELXT using intrinsic phasing and were refined with SHELXL using least squares minimization.[3-5] All non-hydrogen atoms were refined anisotropically. All hydrogen atom positions were calculated geometrically and refined using the riding model. Crystallographic data, refinement details are given in Tables S1-S4.

Table S1. Crystal Data and Structure Refinement for **1** and **2**.

Compound reference	**1**	**2**
Chemical formula	$C_{136}H_{116}B_2Cl_8Dy_2F_4N_{12}$	$C_{135}H_{114}B_2Cl_6Dy_2F_4N_{12}$
Formula Mass	2624.62	2539.70
Temperature (K)	180	180
Crystal system	orthorhombic	orthorhombic
Space group	$P2_12_12_1$	$P2_12_12_1$
a (Å)	17.2123 (5)	17.2406 (6)
b (Å)	25.8184 (6)	25.9357 (10)
c (Å)	27.5581 (8)	27.5500 (12)
α (°)	90	90
β (°)	90	90
γ(°)	90	90
Unit cell volume (Å^3)	12246.7 (6)	12318.9 (8)
Z	4	4
ρ_{calc} (g/cm^3)	1.424	1.369
μ / mm^{-1}	1.447	1.394
F (000)	5320	5152
Radiation	MoKα (λ = 0.71073)	MoKα (λ = 0.71073)
Reflections collected	91773	80204
Independent reflections	21639	21727
R_{int}	0.1061	0.0935
GOF on F^2	1.065	1.056
R_1 ($I \geq 2\sigma(I)$)	0.0544	0.0500
wR_2 (all data)	0.1403	0.1244
Flack parameter	0.002(6)	0.001(6)
CCDC number	2178369	2178368

Table S2. The CShM values calculated by SHAPE 2.1 for **1** and **2**. The lowest CShM value is highlighted by red color.[6, 7]

Coordination Geometry	**1**		**2**	
	Dy1	**Dy2**	**Dy1**	**Dy2**
Enneagon (D_{9h})	32.975	32.422	32.899	32.392
Octagonal pyramid (C_{8v})	22.328	22.339	22.272	22.283
Heptagonal bipyramid (D_{7h})	14.743	14.784	14.693	14.841
Johnson triangular cupola J3 (C_{3v})	14.330	13.479	14.245	13.410
Capped cube J8 (C_{4v})	8.272	8.528	8.265	8.579
Spherical-relaxed capped cube (C_{4v})	7.213	7.751	7.220	7.802
Capped square antiprism J10 (C_{4v})	7.884	9.192	7.902	9.264
Spherical capped square antiprism (C_{4v})	6.913	8.206	6.943	8.264
Tricapped trigonal prism J51 (D_{3h})	7.315	8.280	7.339	8.349
Spherical tricapped trigonal prism (D_{3h})	7.916	9.287	7.959	9.369
Tridiminished icosahedron J63 (C_{3v})	8.754	8.424	8.673	8.445
Hula-hoop (C_{2v})	2.944	2.714	2.956	2.684
Muffin (C_s)	5.044	6.164	5.075	6.195

Table S3. Selected bond distances (Å) for **1** and **2**.

1	**2**
Dy1-F1 2.264(8)	Dy1-F1 2.102(6)
Dy1-F2 2.268(6)	Dy1-F2 2.270(5)
Dy1-F3 2.267(6)	Dy1-F3 2.271(6)
Dy1-N1 2.630(9)	Dy1-N1 2.640(8)
Dy1-N2 2.654(10)	Dy1-N2 2.684(8)
Dy1-N3 2.659(10)	Dy1-N3 2.648(9)
Dy1-N4 2.635(10)	Dy1-N4 2.629(9)
Dy1-N5 2.657(9)	Dy1-N5 2.658(9)
Dy1-N6 2.626(10)	Dy1-N6 2.652(8)
Dy2-F2 2.271(6)	Dy2-F2 2.282(5)
Dy2-F3 2.262(6)	Dy2-F3 2.256(5)
Dy2-F4 2.105(7)	Dy2-F4 2.266(7)
Dy2-N7 2.672(9)	Dy2-N7 2.669(10
Dy2-N8 2.639(10)	Dy2-N8 2.650(9)
Dy2-N9 2.661(9)	Dy2-N9 2.629(9)
Dy2-N10 2.706(10)	Dy2-N10 2.621(9)
Dy2-N11 2.660(10)	Dy2-N11 2.677(8)
Dy2-N12 2.646(9)	Dy2-N12 2.637(9)

Table S4. Selected bond angles (°) for **1** and **2**.

1	**2**
Dy1-F2-Dy2 114.1(3)	Dy1-F2-Dy2 113.6(2)
Dy1-F3-Dy2 114.4(3)	Dy1-F3-Dy2 114.5(2)
F1-Dy1-F2 144.9(2)	F1-Dy1-F2 147.7(2)
F1-Dy1-F3 149.1(2)	F1-Dy1-F3 146.4(0)
F1-Dy1-N1 73.0(3)	F1-Dy1-N1 73.8(3)
F1-Dy1-N2 81.3(3)	F1-Dy1-N2 80.2(3)
F1-Dy1-N3 94.6(3)	F1-Dy1-N3 90.4(3)
F1-Dy1-N4 73.4(3)	F1-Dy1-N4 74.3(3)
F1-Dy1-N5 77.0(3)	F1-Dy1-N5 80.9(3)
F1-Dy1-N6 89.8(3)	F1-Dy1-N6 91.2(3)
F2-Dy1-F3 65.7(2)	F2-Dy1-F3 65.93(18)
F2-Dy1-N1 129.7(3)	F2-Dy1-N1 126.5(3)
F2-Dy1-N2 131.5(3)	F2-Dy1-N2 130.4(2)
F2-Dy1-N3 93.4(3)	F2-Dy1-N3 96.9(2)
F2-Dy1-N4 81.2(3)	F2-Dy1-N4 82.2(3)
F2-Dy1-N5 69.5(3)	F2-Dy1-N5 68.2(2)
F2-Dy1-N6 82.7(3)	F2-Dy1-N6 81.2(3)
F3-Dy1-N1 80.7(3)	F3-Dy1-N1 81.2(3)
F3-Dy1-N2 71.7(3)	F3-Dy1-N2 68.0(2)
F3-Dy1-N3 84.8(3)	F3-Dy1-N3 83.2(3)
F3-Dy1-N4 130.3(3)	F3-Dy1-N4 128.0(3)
F3-Dy1-N5 129.6(3)	F3-Dy1-N5 130.4(3)
F3-Dy1-N6 91.6(3)	F3-Dy1-N6 95.9(3)
N1-Dy1-N2 60.8(3)	N1-Dy1-N2 61.1(3)
N1-Dy1-N3 120.7(3)	N1-Dy1-N3 120.6(3)
N1-Dy1-N4 146.4(3)	N1-Dy1-N4 148.1(3)
N1-Dy1-N5 112.9(3)	N1-Dy1-N5 113.0(3)
N1-Dy1-N6 61.1(3)	N1-Dy1-N6 60.7(3)
N2-Dy1-N3 60.0(3)	N2-Dy1-N3 60.0(2)
N2-Dy1-N4 111.7(3)	N2-Dy1-N4 113.7(3)

N2-Dy1-N5 158.2(3)	N2-Dy1-N5 161.1(3)
N2-Dy1-N6 121.3(3)	N2-Dy1-N6 121.2(3)
N3-Dy1-N4 60.3(3)	N3-Dy1-N4 60.2(3)
N3-Dy1-N5 120.3(3)	N3-Dy1-N5 120.4(3)
N3-Dy1-N6 175.6(3)	N3-Dy1-N6 178.1(3)
N4-Dy1-N5 60.7(3)	N4-Dy1-N5 60.7(3)
N4-Dy1-N6 120.9(3)	N4-Dy1-N6 119.5(3)
N5-Dy1-N6 60.3(3)	N5-Dy1-N6 59.0(3)
F4-Dy2-F2 148.2(3)	F2-Dy2-F3 65.98(18)
F4-Dy2-F3 146.0(3)	F2-Dy2-F4 144.9(2)
F4-Dy2-N7 80.2(3)	F2-Dy2-N7 93.7(3)
F4-Dy2-N8 73.8(3)	F2-Dy2-N8 131.5(2)
F4-Dy2-N9 91.4(3)	F2-Dy2-N9 130.0(3)
F4-Dy2-N10 80.9(3)	F2-Dy2-N10 82.4(3)
F4-Dy2-N11 74.3(3)	F2-Dy2-N11 69.1(2)
F4-Dy2-N12 90.5(3)	F2-Dy2-N12 81.7(3)
F2-Dy2-F3 65.7(2)	F3-Dy2-F4 148.9(2)
F2-Dy2-N7 130.0(3)	F3-Dy2-N7 84.7(3)
F2-Dy2-N8 126.3(3)	F3-Dy2-N8 71.4(3)
F2-Dy2-N9 80.9(3)	F3-Dy2-N9 80.9(2)
F2-Dy2-N10 68.7(3)	F3-Dy2-N10 91.8(3)
F2-Dy2-N11 82.4(3)	F3-Dy2-N11 129.4(2)
F2-Dy2-N12 96.8(3)	F3-Dy2-N12 130.5(3)
F3-Dy2-N7 67.6(3)	F4-Dy2-N7 94.1(2)
F3-Dy2-N8 80.8(3)	F4-Dy2-N8 81.3(2)
F3-Dy2-N9 95.9(3)	F4-Dy2-N9 72.9(2)
F3-Dy2-N10 130.7(3)	F4-Dy2-N10 90.2(3)
F3-Dy2-N11 128.6(3)	F4-Dy2-N11 77.4(2)
F3-Dy2-N12 83.2(3)	F4-Dy2-N12 72.9(2)
N7-Dy2-N8 60.5(3)	N7-Dy2-N8 59.7(3)
N7-Dy2-N9 121.2(3)	N7-Dy2-N9 120.3(3)
N7-Dy2-N10 161.1(3)	N7-Dy2-N10 175.6(3)
N7-Dy2-N11 114.6(3)	N7-Dy2-N11 120.6(3)
N7-Dy2-N12 60.3(3)	N7-Dy2-N12 60.1(3)
N8-Dy2-N9 61.2(3)	N8-Dy2-N9 60.8(3)
N8-Dy2-N10 113.1(3)	N8-Dy2-N10 121.6(3)
N8-Dy2-N11 148.1(3)	N8-Dy2-N11 158.7(3)
N8-Dy2-N12 120.5(3)	N8-Dy2-N12 111.2(3)
N9-Dy2-N10 58.7(3)	N9-Dy2-N10 61.5(3)
N9-Dy2-N11 118.6(3)	N9-Dy2-N11 112.9(3)
N9-Dy2-N12 177.7(3)	N9-Dy2-N12 145.7(3)
N10-Dy2-N11 60.2(3)	N10-Dy2-N11 59.9(3)
N10-Dy2-N12 120.5(3)	N10-Dy2-N12 121.1(3)
N11-Dy2-N12 60.8(3)	N11-Dy2-N12 61.3(3)

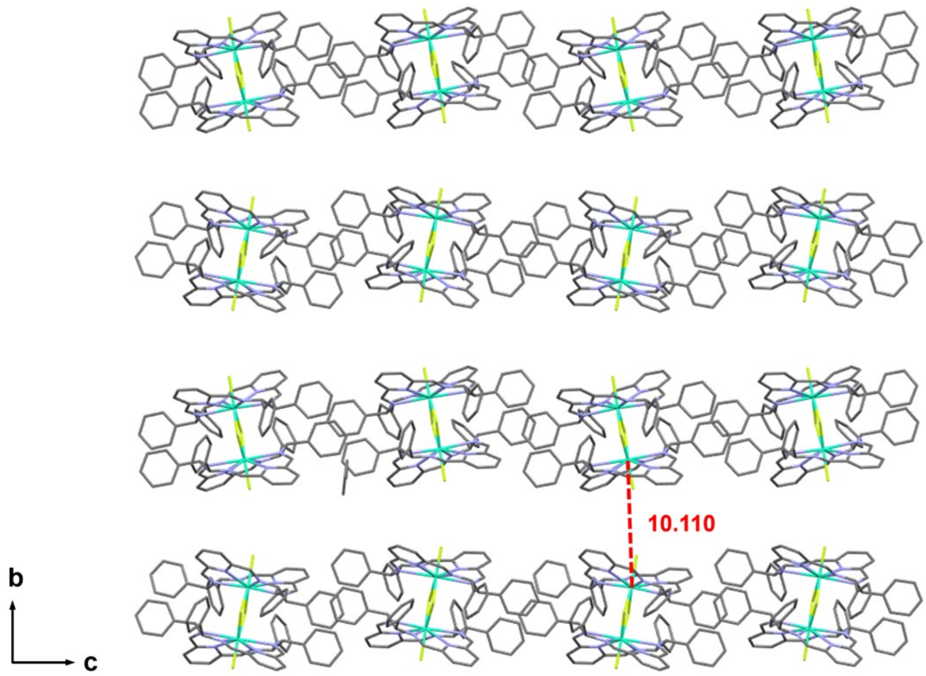

Fig. S4 The packing diagram for **1** gives the shortest intermolecular Dy···Dy distance of 10.110 Å.

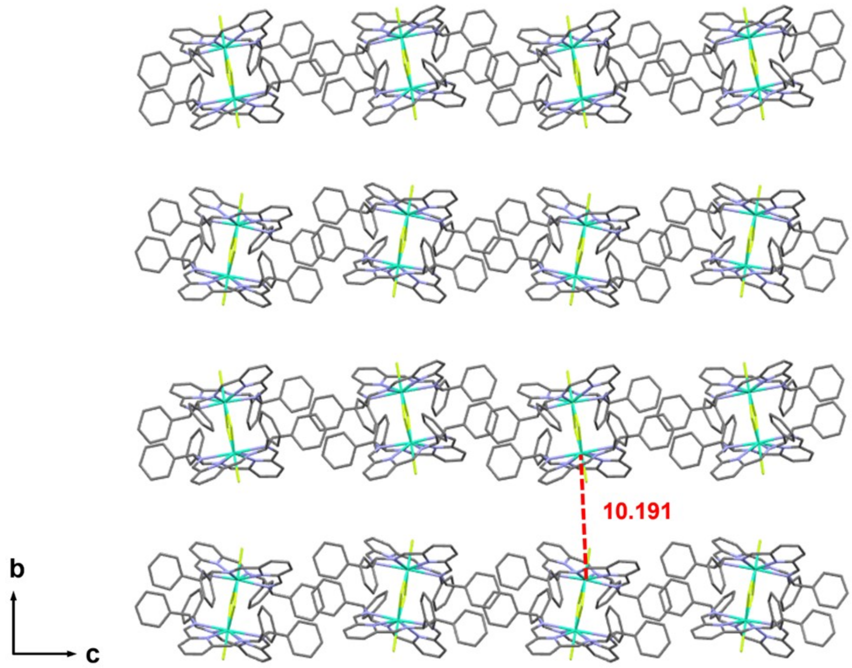

Fig. S5 The packing diagram for **2** gives the shortest intermolecular Dy···Dy distance of 10.191 Å.

3. Magnetic measurements

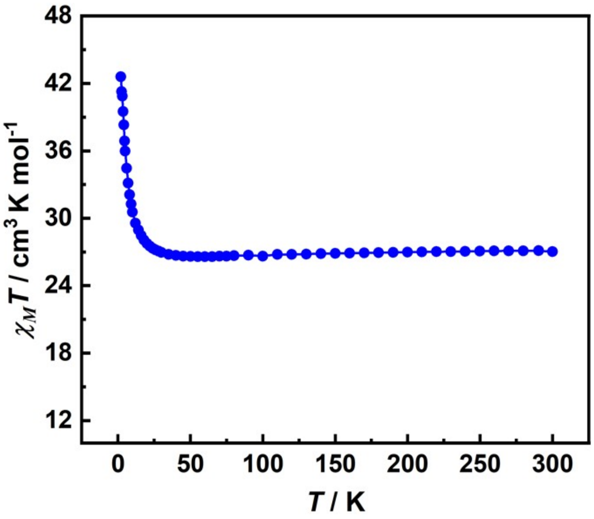

Fig. S6 $\chi_M T$ vs. T plot of **1**.

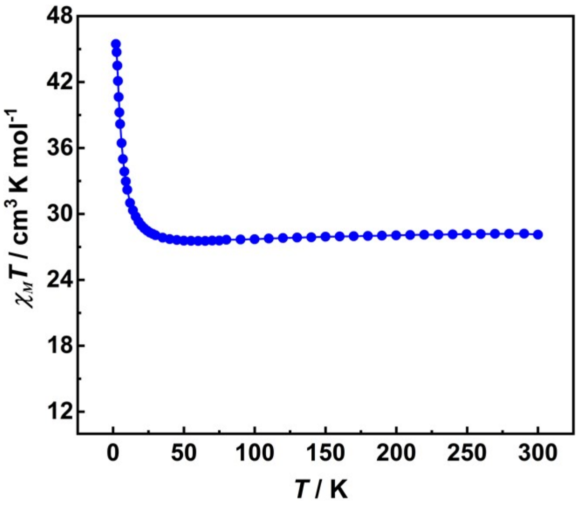

Fig. S7 $\chi_M T$ vs. T plot of **2**.

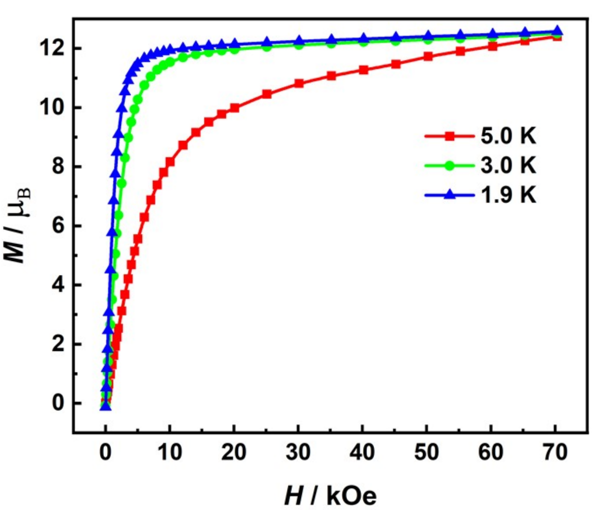

Fig. S8 Field dependence of the magnetization at 1.9, 3 and 5 K for **1**.

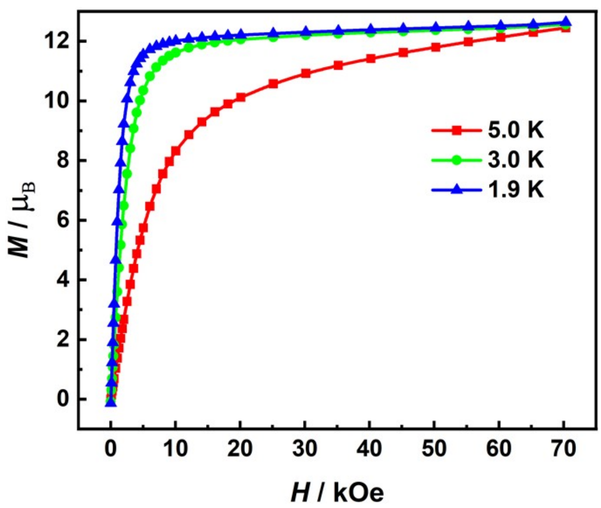

Fig. S9 Field dependence of the magnetization at 1.9, 3 and 5 K for **2**.

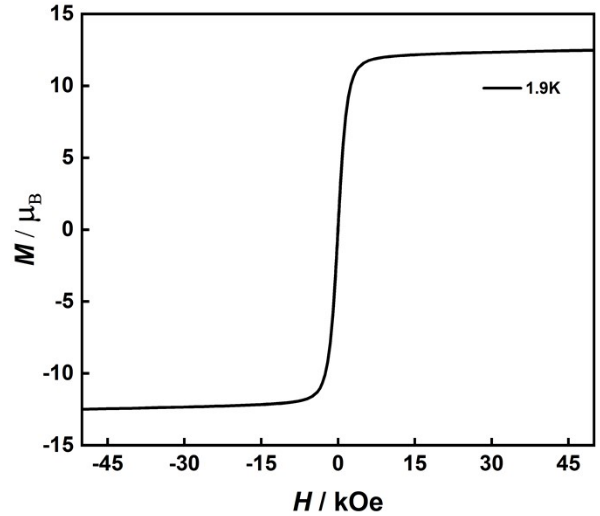

Fig. S10 Magnetic hysteresis of solid **1** at 1.9 K using an average sweep rate of 31 Oe/s.

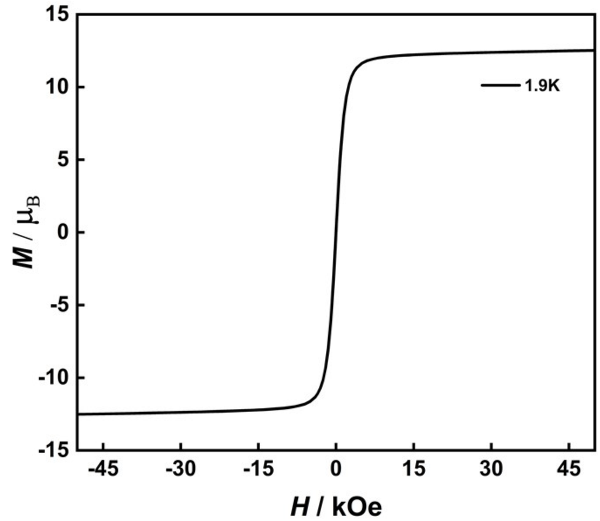

Fig. S11 Magnetic hysteresis of solid **2** at 1.9 K using an average sweep rate of 31 Oe/s.

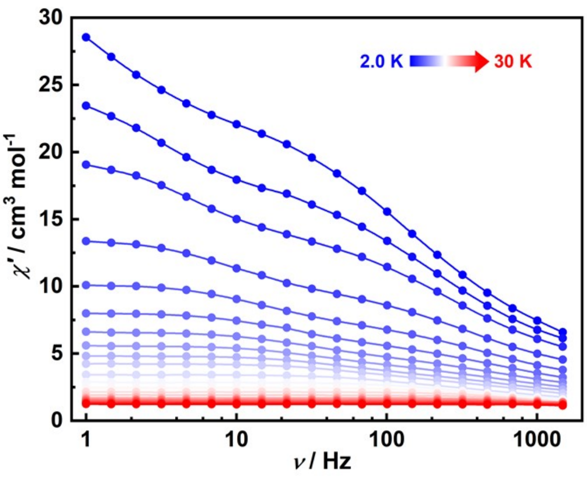

Fig. S12 Frequency dependence of the in-phase susceptibility (χ') for **1** under a zero dc field at ac frequencies of 1-1488 Hz in the temperature range of 2 to 30 K.

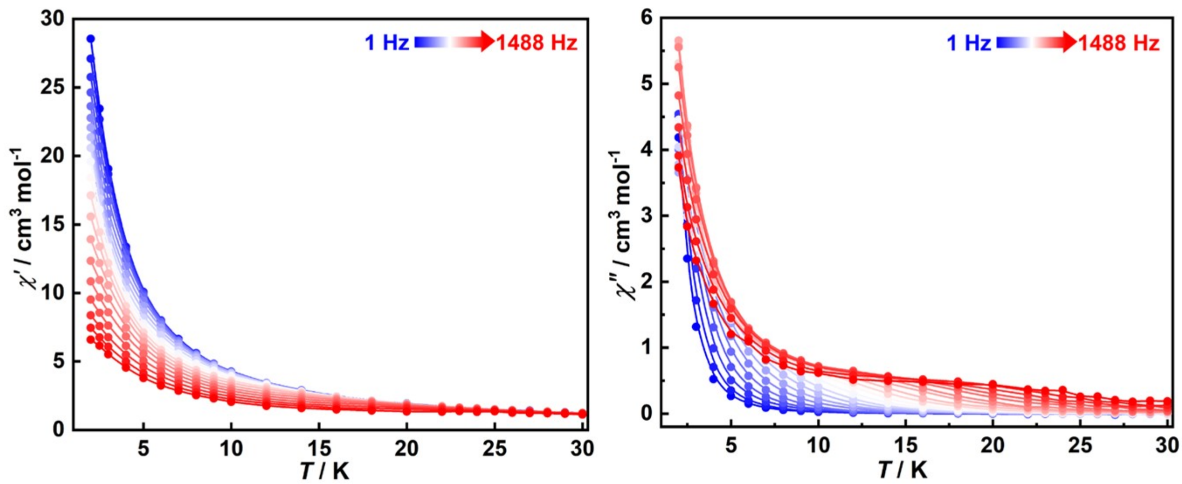

Fig. S13 Temperature dependence of the in-phase (left) and out-of-phase (right) susceptibility for **1** under a zero dc field in ac frequencies of 1-1488 Hz.

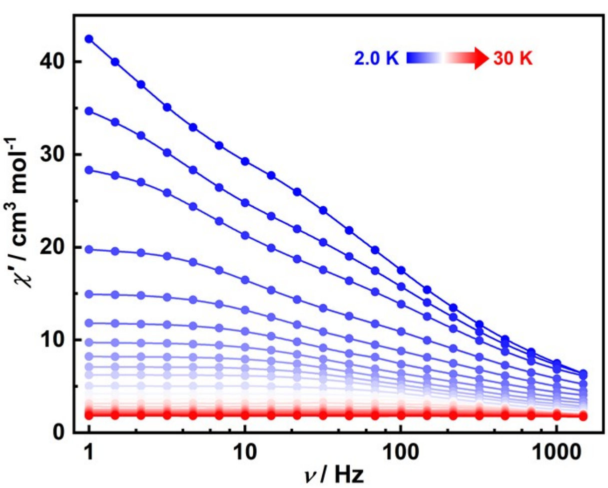

Fig. S14 Frequency dependence of the in-phase susceptibility (χ') for **2** under zero dc field at ac frequencies of 1-1488 Hz in the temperature range of 2 to 30 K.

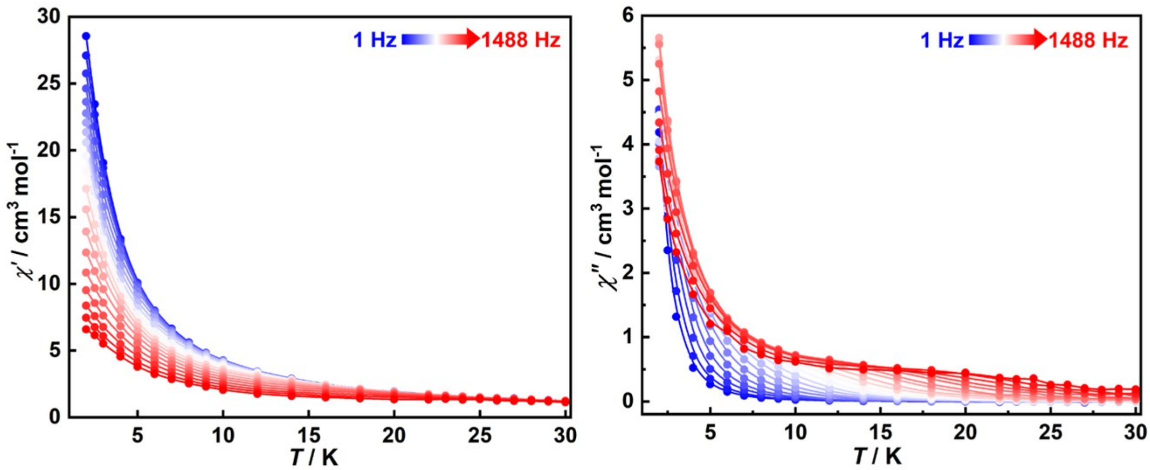

Fig. S15 Temperature dependence of the in-phase (left) and out-of-phase (right) susceptibility for **2** under a zero dc field in ac frequencies of 1-1488 Hz.

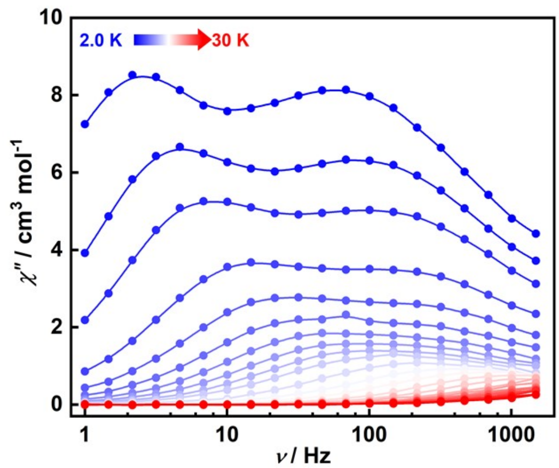

Fig. S16 Frequency dependence of the out-of-phase susceptibility (χ'') for **2** under a zero dc field at ac frequencies of 1-1488 Hz in the temperature range of 2 to 30 K.

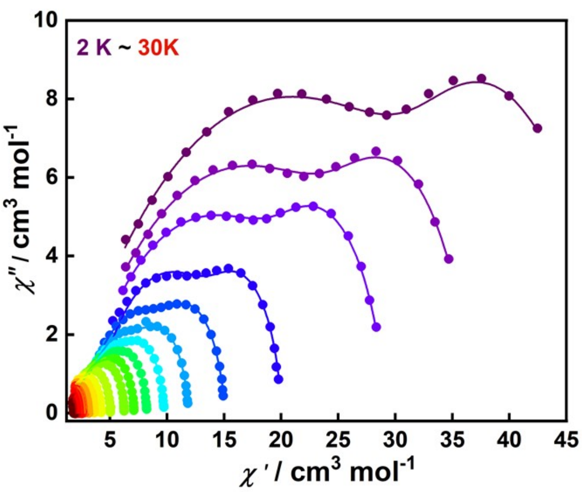

Fig. S17 Cole-Cole plot for **2**. The solid lines are obtained by fitting experimental data with CC-FIT2.[8]

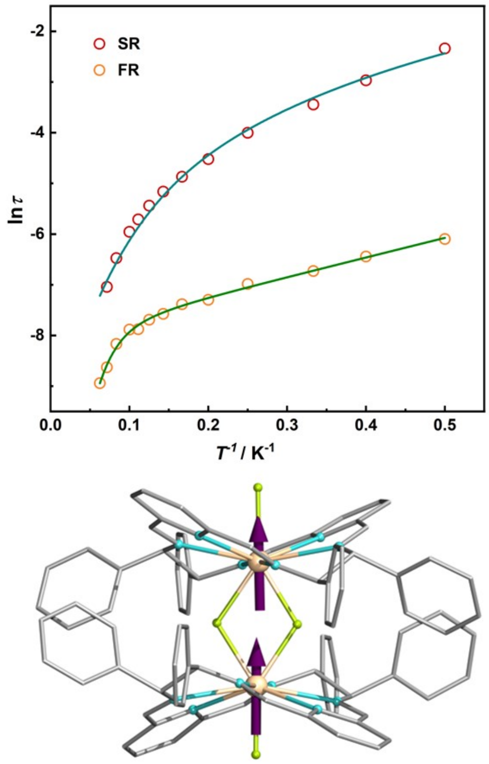

Fig. S18 (Top) Temperature-dependent relaxation time for **2**. The solid lines represent the fitting with parameters of U_{eff} = 26(2) cm^{-1}, τ_0= 10$^{-3.5(3)}$ s, C = 2.5(6) s^{-1} K^{-n}, n = 2.2(2) for the SR process and U_{eff} = 3.0(1) cm^{-1}, τ_0= 10$^{-3.5(1)}$ s, C = 0.05(7) s^{-1} K^{-n}, n = 4.2(5) for the FR process. (Bottom) The purple rows represent the orientation of the anisotropy axis of the individual Dy(III) in **2** as calculated by Magellan software.[9]

4. References

1. C. Zhao, Z. Zhu, X.-L. Li and J. Tang, Inorg. Chem. Front., 2022, **9**, 4049-4055.
2. E. A. Boudreaux and L. N. Mulay, *John Wiley & Sons: New York*, 1976.
3. O. V. Dolomanov, L. J. Bourhis, R. J. Gildea, J. A. K. Howard and H. Puschmann, *J. Appl. Crystallogr.*, 2009, **42**, 339-341.
4. G. M. Sheldrick, *Acta Crystallogr. Sect. C-Struct. Chem.*, 2015, **71**, 3-8.
5. G. M. Sheldrick, *Acta Crystallogr. Sect. A*, 2015, **71**, 3-8.
6. M. Pinsky and D. Avnir, *Inorg. Chem.*, 1998, **37**, 5575-5582.
7. D. Casanova, J. Cirera, M. Llunell, P. Alemany, D. Avnir and S. Alvarez, *J. Am. Chem. Soc.*, 2004, **126**, 1755-1763.
8. D. Reta and N. F. Chilton, *Phys. Chem. Chem. Phys.*, 2019, **21**, 23567-23575.
9. N. F. Chilton, D. Collison, E. J. McInnes, R. E. Winpenny and A. Soncini, *Nat. Commun.*, 2013, **4**, 2551.